JAAS FULL PAPER
www.rsc.org/jaas

Improved hybrid Monte Carlo–fluid model for the electrical characteristics in an analytical radio-frequency glow discharge in argon

Annemie Bogaerts,*[a] Renaat Gijbels[a] and Wim Goedheer[b]

[a]*Department of Chemistry, University of Antwerp, Universiteitsplein 1, B-2610 Wilrijk-Antwerp, Belgium*
[b]*FOM-Institute for Plasma Physics "Rijnhuizen", P.O. Box 1207, 3430 BE Nieuwegein, The Netherlands*

Received 26th April 2001, Accepted 16th May 2001
First published as an Advance Article on the web 19th June 2001

An improved hybrid Monte Carlo–fluid model for electrons, argon ions and fast argon atoms, is presented for the rf Grimm-type glow discharge. In this new approach, all electrons, including the large slow electron group in the bulk plasma, are treated with the Monte Carlo model. The calculation results presented here are the electrical characteristics (voltage, current and power as a function of time in the rf cycle, as well as the electrical potential and field distribution in the discharge), the electron and argon ion densities, and the electron, fast argon ion and atom impact ionization rates. In particular, the newly calculated electron impact ionization rate is more reliable now, because it is explicitly calculated in the electron Monte Carlo model instead of using an approximate formula, as in the earlier fluid model. Consequently, the major difference with our previous calculation results is found in the electron impact ionization rate. The calculated electrical characteristics (voltage, current and power) are, however, very similar to the results of our previous model. The new model confirms that the plasma displacement current is lower than the ion and electron conduction currents at the typical analytical rf Grimm-type glow discharge conditions, and therefore that the plasma current and voltage are in phase with each other. This is in contrast to other modeling results published recently, but in agreement with experimental observations where the capacitive current of the measuring circuit had also been subtracted from the total current.

1. Introduction

Rf powered GD-OES is becoming a well-established method, mainly for the analysis of non-conductive materials.[1,2] However, the rf glow discharge is not yet fully understood, and a better characterization, both by modeling and experiments, is desirable for improved analytical practice. Indeed, the experimental determination of the electrical characteristics (voltage and current as a function of time, as well as the electrical power effectively going into the discharge) is far from straightforward.[3,4] On the other hand, the models developed up to now to obtain a better understanding do not present a unified picture of the rf glow discharge.[5–7]

In the rf model that we originally developed,[5] all electrons starting from the rf electrode (due to secondary electron emission) and the ones created by ionization in the plasma, were simulated with a Monte Carlo method, irrespective of their energy. However, a model comparison between a dc and an rf discharge revealed that the rf discharge yielded less ionization, and hence required higher voltages (rf amplitude and dc bias voltage) for the same values of pressure and power as the dc discharge, which was in contrast to experimental observations, where the opposite is generally found.[8] This suggested that the behavior of the electrons and their ionization mechanisms were not correctly described in that rf model. Indeed, in general in the rf mode, the slow electrons can become heated again by the fluctuating rf electric field, and they can again give rise to ionization (*i.e.*, so-called alpha-ionization).[9] It appears that the electron density, calculated in the Monte Carlo model, was lower than the density predicted from the fluid code (based on the electric field distribution and the Poisson equation), which means that the slow electron group, and therefore also their contribution to ionization (after being heated by the fluctuating rf field, *i.e.*, alpha-ionization, or by the moderate bulk electric field at $\omega t = \pi/2$), were underestimated in the rf model. Several attempts to describe this large group of slow electrons (which will be built up after a very long time, from the avalanche of the electrons starting at the rf electrode) in the Monte Carlo code failed, mainly due to extremely long calculation times. Therefore, in the second version of our rf model, the slow electrons were treated in the fluid model; they were allowed to be heated by the fluctuating rf field, and they could give rise to ionization. The latter, *i.e.*, alpha-ionization, was described in the fluid code by a simple empirical formula for the ionization rate as a function of the mean electron energy, which was also calculated in the fluid code.[6] With this new model, the comparison of electrical characteristics (voltage, current, power) between a dc and an rf discharge yielded reasonable agreement with the experimental data.[10] However, it should be mentioned that both the calculations of the ionization rate and of the mean electron energy in the fluid code are only an approximation, which had to be accepted to avoid the long computation times.

Moreover, beside these difficulties encountered in our own rf models, a paper by Belenguer *et al.* has recently been published,[7] which shows discrepancies with our results. Indeed, by using a hybrid Monte Carlo–fluid model (but treating all electrons with the Monte Carlo method, and not describing the fast argon ions and atoms with a Monte Carlo method), the authors found that the rf glow discharge used for GD-OES has a capacitive electrical behavior (*i.e.*, voltage and current out of phase by $\pi/2$ with respect to each other) which appeared to arise from a dominant contribution of the displacement current to the overall electrical current,[7] whereas we found, in both

 DOI: 10.1039/b103768b

versions of our rf model,[5,6] that the displacement current was of minor importance at typical analytical operating conditions, and consequently that the Grimm-type rf glow discharge has a resistive character (*i.e.*, voltage and current in phase with each other).

This discrepancy between our model results and the results of Belenguer *et al.* (who have a long experience with the modeling of rf glow discharges for technological applications), as well as the serious approximation that we had to carry out in our second version of the rf model (*i.e.*, alpha-ionization treated with the fluid model) were the driving forces for us to develop a new, improved rf model for the electrical characteristics in the Grimm-type glow discharge cell in argon. In section 2, this improved model will be explained. It will, however, be demonstrated in section 3 that this improved model predicts a resistive character of the rf analytical glow discharge, and that the plasma displacement current is still lower than the ion and electron conduction currents. The calculation of the plasma displacement current will be illustrated in more detail from the variation of the calculated electric field at the rf electrode.

2. Description of the model

The species assumed to be present in the model for the electrical characteristics of the rf glow discharge are the argon gas atoms, electrons, argon ions and fast argon atoms (which are created from collisions of the argon ions in the sheath). The other plasma species (argon excited atoms, sputtered atoms and ions) are of minor importance for the electrical characteristics and are not incorporated here.

The argon gas atoms are not described explicitly in a model, because they are assumed to be uniformly distributed in the plasma and at thermal energies. The behavior of electrons, argon ions and fast argon atoms is calculated in a hybrid Monte Carlo–fluid model. As mentioned above, all electrons are treated with the Monte Carlo method. Additionally, the fluid model calculates the density of electrons and argon ions, based on the ionization rates calculated in the Monte Carlo model. Moreover, the fluid model also contains Poisson's equation, in order to calculate the electric field distribution from the argon ion and electron densities. In principle, the electrons do not have to be treated additionally with the fluid model, but it appeared to be numerically more simple to maintain the three coupled differential equations (*i.e.*, electron continuity equation, ion continuity equation and Poisson's equation[5,6]) in the fluid code. Hence, this means that the electrons are treated simultaneously in two models: a Monte Carlo model and a fluid model. The Monte Carlo model is especially important to yield the accurate electron impact ionization rates (used as input in the fluid model) whereas the fluid model is used to calculate the electron density, coupled to Poisson's equation.

As well as the electron Monte Carlo model, the argon ions and fast argon atoms are also treated with a Monte Carlo model, but only in the sheath region adjacent to the rf electrode. Indeed, these species can have rather higher energies in the sheath, especially for high discharge voltages, and they give rise to additional ionization (*i.e.*, fast argon ion and atom impact ionization),[11] which is also used as input for the argon ion and electron creation rates in the fluid model.

The principles of the electron, fast argon ion and atom Monte Carlo models, of the electron–argon ion fluid model, and of the coupling of the three models, are in most cases similar to our dc hybrid model and previous rf models, and detailed information can be found in refs. 12 (dc hybrid model and coupling) and 5, 6 and 11 (specific features of the rf model, *e.g.*, time-dependence of the plasma quantities). The only and major difference, as mentioned above, is the treatment of all electrons with the Monte Carlo method, which is explained below in some more detail.

In the hybrid Monte Carlo–fluid model described in ref. 5, all electrons were treated with the Monte Carlo method, but it appeared that the slow electron group was not correctly described. Indeed, the Monte Carlo model simulated the behavior of electrons created at the rf electrode (from secondary electron emission) and the electrons created by ionization of these gamma-electrons (*i.e.*, the so-called avalanche electrons). But it takes a very long time before the avalanche electrons have built up into the large population of slow electrons, and it appeared that the Monte Carlo model of ref. 5 did not treat all these slow electrons in a proper way. In the present Monte Carlo model, we have overcome this problem of extremely long calculation times before the slow electron group is built up (typical computation times of several days on a professional workstation). Indeed, the slow electron group is introduced now at time-step $t = 0$ in the Monte Carlo model, from the fluid calculations. Most of these electrons will remain slow and do not contribute to the ionization. However, a fraction of them will be sufficiently heated to produce alpha-ionization. In this way, all electrons, including the slow ones, are correctly treated in the Monte Carlo model, within a reasonable time-scale (less than one day, for sufficient statistics). Moreover, in order to further reduce the calculation time, a method of combining the slow electrons into a lower number of "super-electrons" with a higher weight factor is applied, based on the procedure described in ref. 13. If the electrons in the bulk plasma have energies lower than the threshold for inelastic collisions (*i.e.*, 11.55 eV, in the case of argon), a fraction defined by the parameter "ftoss" will be removed from the Monte Carlo model. Therefore, a random number (RN) between 0 and 1 is generated. If ftoss $>$ RN, the electron is removed. If ftoss $<$ RN, the electron remains in the model, and since the real number of electrons must be constant, there must be a compensation for those which disappear; hence the weight of the electrons which remain in the plasma is increased by: $w = w/(1 - \text{ftoss})$. It is clear that a higher value for ftoss will result in a more efficient reduction in the computation time, but, on the other hand, a too high value will affect the statistics of the Monte Carlo model. In principle, this method might cause a deviation in the electron energy distribution, because only low-energy electrons are removed. However, by increasing the weight of the low-energy electrons (see above), this effect should be sufficiently compensated for, as long as the value of ftoss is not too high. In practice, we found that a value equal to 0.001 yielded satisfactory and statistically valid results within a reasonable computation time (typically several hours to one day, depending on the statistics).

3. Results and discussion

3.1. Electrical characteristics

The calculations are performed for the same conditions as in ref. 6, in order to check the effect of treating all electrons with the Monte Carlo method (compared to the approximation made in ref. 6 by treating the slow electrons and alpha-ionization with the fluid model). Moreover, the relative contribution of the plasma displacement current will also be investigated in more detail for these discharge conditions.

The input values in the model are 5.775 Torr gas pressure and 10.2 W electrical power. The voltage and current as a function of time in the rf cycle are then calculated. Moreover, a value of the gas temperature has to be used as input value. Because this value is actually unknown, we used it as a kind of fitting parameter in the model, in order to obtain calculated voltages (rf amplitude and dc bias) in agreement with the measured data. The cell geometry under study is a simple cylinder of 2.5 mm diameter and 2 cm length, which is a

reasonable simplification of the Grimm-type source with the anode diameter adjacent to the rf electrode equal to 2.5 mm, because the discharge is concentrated in the first cm adjacent to the rf electrode or cathode.[14]

Fig. 1 shows the calculated voltage as a function of time in the rf cycle, for the conditions given above. This figure looks quite similar to Fig. 1a of ref. 6, which showed the time-behavior of the voltage, calculated with our previous version of the model. The voltage appears to be negative during most of the rf cycle. This is due to the highly negative dc bias (see figure), which arises from the large difference in size between the rf powered and grounded electrode. We calculated here an rf amplitude (V_{rf}) of 741 V and a dc bias ($V_{dc\text{-}bias}$) of −658 V. With the previous rf model, these values were calculated to be $V_{rf} = 937$ V and $V_{dc\text{-}bias} = -640$ V, respectively.[6] The experimental values, for the same conditions of pressure and power (see dashed line in Fig. 1), are $V_{rf} = 764$ V and $V_{dc\text{-}bias} = -627$ V.[6] Hence, it appears that our previous calculations predicted a value for V_{rf} somewhat too high, whereas the value for $V_{dc\text{-}bias}$ was more or less correct (slightly too high). The difference between V_{rf} and $V_{dc\text{-}bias}$, which determines the positive value of the voltage at $\omega t = \pi/2$, was about 300 V, which is higher than the experimental value (*i.e.*, 137 V). The present calculations, on the other hand, yield a value of $V_{dc\text{-}bias}$ slightly too high, and a value of V_{rf} slightly too low. Therefore, the difference between V_{rf} and $V_{dc\text{-}bias}$ (*i.e.*, 83 V) was somewhat too low, but in slightly better agreement with the experimental difference. This illustrates how difficult it is to obtain exact agreement with experimental values (also because the measured dc bias voltage might be subject to uncertainties), but nevertheless, the present correspondence is considered to be satisfactory (see solid and dashed lines in Fig. 1).

Fig. 2 shows the one-dimensional potential distribution throughout the discharge (at the cell axis) at four times in the rf cycle. The potential at the rf electrode is highly negative at $\omega t = \pi$, $3\pi/2$ and 2π (see the enlarged part in Fig. 2), as follows also from Fig. 1. Indeed, it is equal to $V_{dc\text{-}bias}$ (−658 V) at $\omega t = \pi$ and 2π, and it is equal to $-V_{rf} + V_{dc\text{-}bias}$ (= −1400 V) at $\omega t = 3\pi/2$. The potential increases rapidly as a function of distance from the rf electrode. It goes through zero at about 0.5 mm from the rf electrode, and is slightly positive (*ca.* 36 V at the maximum) in the bulk plasma, before it returns to zero at the grounded wall ($z = 2$ cm). At $\omega t = \pi/2$, a completely different potential distribution is shown, *i.e.*, the potential is positive at the rf electrode ($V_{rf} + V_{dc\text{-}bias} = 83$ V) and it returns gradually to zero at the grounded wall. Fig. 2 is again quite similar to Fig. 2 of ref. 6, except that the potential at $\omega t = \pi/2$ is now somewhat lower than in ref. 6, which follows of course from the smaller difference between V_{rf} and $V_{dc\text{-}bias}$. In reality, the potential at $\omega t = \pi/2$ will probably be between both values, *i.e.*, equal to the experimental potential difference (measured to be 137 V).

From the potential distribution, the electric field (E_f) can easily be calculated, since $E_f = -\text{grad}(V)$. The result is presented in Fig. 3, at four times during the rf cycle. The electric field is very negative at $\omega t = \pi$, $3\pi/2$ and 2π (*i.e.*, about -23 kV cm^{-1} at $\omega t = \pi$, -38 kV cm^{-1} at $\omega t = 3\pi/2$, and -27 kV cm^{-1} at $\omega t = 2\pi$; see the enlarged part in Fig. 3). It increases however very rapidly and bends off to low values at less than 1 mm from the rf electrode. At $\omega t = \pi/2$, the electric field at the rf electrode has a positive value of about 1.5 kV cm^{-1}, which is very low compared to the other times. In the bulk plasma, *i.e.*, at distances further than 1–2 mm from the rf electrode, the electric field ranges between 1 and 70 V cm^{-1}, and is similar at all times in the rf cycle. These slightly positive values are the result of the small drop of the potential as a function of distance (see Fig. 2). Fig. 3 is again very similar to Fig. 3 in ref. 6, except for the electric field in the bulk plasma at $\omega t = \pi/2$. Indeed, the latter is somewhat lower in the new results, which is of course again due to the smaller difference between V_{rf} and $V_{dc\text{-}bias}$, and hence the lower potential at the rf electrode at $\omega t = \pi/2$.

Fig. 4 shows the calculated electrical current as a function of

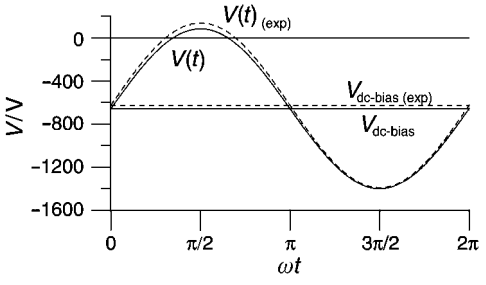

Fig. 1 Calculated (solid line) and experimental (dashed line) voltage at the rf electrode as a function of time in the rf cycle, at 5.775 Torr and 10.2 W. Also shown are the calculated and experimental dc bias voltages ($V_{dc\text{-}bias}$; solid and dashed lines, respectively).

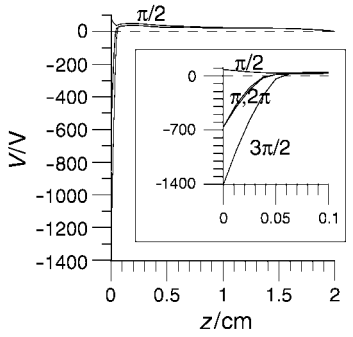

Fig. 2 Calculated potential distribution throughout the discharge, at four times in the rf cycle, for the same discharge conditions as in Fig. 1. The enlarged part in the figure shows the behavior in the rf sheath.

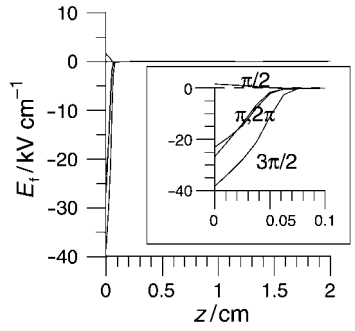

Fig. 3 Calculated electric field distribution throughout the discharge, at four times in the rf cycle, for the same discharge conditions as in Fig. 1. The enlarged part in the figure shows the behavior in the rf sheath.

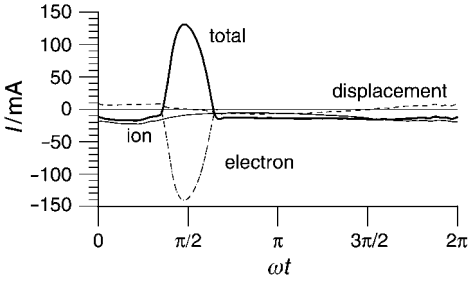

Fig. 4 Calculated electrical current at the rf electrode as a function of time in the rf cycle (thick solid line), as well as contributions of the ion conduction current (thin solid line), the electron conduction current (dash-dotted line) and the displacement current (dashed line), for the same discharge conditions as in Fig. 1.

time in the rf cycle, as well as the contributions of ion and electron conduction currents and of the displacement current. The displacement current arises from the movement of the rf sheath (*i.e.,* it becomes thicker and thinner) as a function of time. Since the rf sheath is characterized by a positive space charge, the movement of the rf sheath results in a change of positive space charge, and hence in an electrical current (since $I = \mathrm{d}q/\mathrm{d}t$, where I, q and t represent the current, electrical charge, and time, respectively). The displacement current density (j_d) is calculated as:[5]

$$j_\mathrm{d} = \varepsilon_0 \frac{\mathrm{d}E_\mathrm{f}}{\mathrm{d}t} \quad (1)$$

where ε_0 and E_f stand for the permittivity in vacuum and the electric field, respectively. By multiplying with the surface area of the rf electrode, one obtains the displacement current, I_d. It appears from Fig. 4 that I_d is again lower than the ion and electron conduction currents. This is in agreement with our previous calculations,[5,6] but in disagreement with the results of Belenguer *et al.*,[7] who calculated a displacement current which is two orders of magnitude higher than the ion and electron conduction currents.[7]

In order to try to understand the discrepancy between our calculation results and the results of ref. 7, we have made a more detailed investigation of the order of magnitude of the displacement current in our calculations. In Fig. 5, the calculated electric field at the rf electrode is presented as a function of time in the rf cycle (solid line, left axis). It is expressed in V m^{-1} (1 V m^{-1} = 10^{-5} kV cm^{-1}), which makes the calculation of I_d more transparent (see below). The values at $\omega t = 0$, $\pi/2$, π, $3\pi/2$ and 2π are given in Table 1. For the calculation of I_d, we need to know $\mathrm{d}E_\mathrm{f}/\mathrm{d}t$. At the frequency of 13.56 MHz, the period of an rf cycle is about 7.4×10^{-8} s; hence, from $\omega t = 0$ to $\pi/2$, $\mathrm{d}t$ is about one quarter of this, *i.e.*, $\mathrm{d}t = 1.85 \times 10^{-8}$ s, and $\mathrm{d}E_\mathrm{f}/\mathrm{d}t$ is about 1.5×10^{14} V m^{-1} s^{-1}. A similar estimate can be made for the other times, and the results are also given in Table 1. The displacement current density, j_d, is obtained from eqn. (1) above. When E_f is expressed in V m^{-1} (1 V m^{-1} = 1 N C^{-1}) and ε_0 is 8.8544×10^{12} C^2 N^{-1} m^{-2}, this gives estimated values for j_d, ranging from -1.15×10^3 to 1.3×10^3 A m^{-2} (see Table 1). Finally, the diameter of the rf electrode is 2.5 mm; hence, the electrode area is about 5×10^{-6} m^2, and the displacement current integrated over the rf electrode, I_d, ranges from -5.8×10^{-3} to 6.5×10^{-3} A, or from -5.8 to 6.5 mA (see Table 1). These estimates are in good agreement with the calculated displacement current as a function of time in the rf cycle, which is illustrated by the dashed line (right axis) in Fig. 5.

It appears that these values of the displacement current are somewhat higher than the results of ref. 6, but they are still lower than the calculated ion conduction current, and than the electron conduction current at $\omega t = \pi/2$. Hence, the total electrical current at the rf electrode [$I = e(I_\mathrm{i} - I_\mathrm{e}) + I_\mathrm{d}$] is still mainly defined by the electron and ion conduction currents. Therefore, it is negative during most of the rf cycle (because the ion conduction current is negative, *i.e.,* directed towards the rf electrode, which is in our simulations situated at $z = 0$), and it becomes only positive around $\omega t = \pi/2$, due to the high electron current directed towards the rf electrode at this time (which is necessary to compensate for the continuous charge accumulation due to the positive ion bombardment).

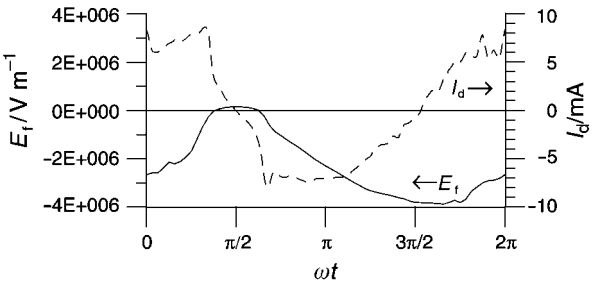

Fig. 5 Calculated electric field at the rf electrode (E_f; in V m^{-1}; solid line, left axis), and calculated displacement current (I_d; in mA; dashed line, right axis), both as a function of time in the rf cycle, for the same discharge conditions as in Fig. 1.

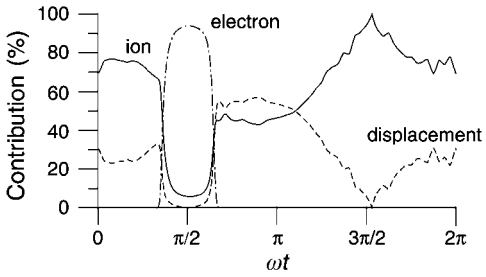

Fig. 6 Calculated relative contributions of the ion conduction current (solid line), the electron conduction current (dash-dotted line) and the displacement current (dashed line), as a function of time in the rf cycle, for the same discharge conditions as in Fig. 1.

Fig. 6 shows the relative contributions of the ion and electron conduction currents and of the displacement current as a function of time in the rf cycle. It is clear that the ion conduction current is dominant during most of the rf cycle, *i.e.*, in the first quarter and the second half of the rf cycle. The electron conduction current is dominant around $\omega t = \pi/2$, as was already illustrated in Fig. 4. The displacement current is only of similar magnitude to the ion conduction current from $\omega t = \pi/2$ to π. However, during this time, it has also a negative sign, so it adds to the ion conduction current, and gives rise to an even more negative total electrical current during this time. During the times when the displacement current has a positive sign, *i.e.*, opposite to the ion conduction current (in the first and the last quarter of the rf cycle), it is of less importance, and therefore it does not give rise to a positive total electrical current.

Finally, by comparing Figs. 1 and 4, it becomes clear that the voltage and current are roughly in phase with each other, in spite of the fact that I_d is $\pi/2$ out of phase with the voltage (see

Table 1 Calculated values of the electric field (E_f) and estimates of the displacement current density (j_d) and displacement current (I_d), at four different times or time ranges in the rf cycle

ωt	0	$\pi/2$	π	$3\pi/2$	2π
E_f/V m^{-1}	-2.7×10^6	1.5×10^5	-2.3×10^6	-3.8×10^6	-2.7×10^6

ωt (range)	From 0 to $\pi/2$	From $\pi/2$ to π	From π to $3\pi/2$	From $3\pi/2$ to 2π
$\mathrm{d}E_\mathrm{f}/\mathrm{d}t$/V m^{-1} s^{-1}	1.5×10^{14}	-1.3×10^{14}	-8×10^{13}	6×10^{13}
j_d/A m^{-2}	1.3×10^3	-1.15×10^3	-7×10^2	5.3×10^2
I_d/A	6.5×10^{-3}	-5.8×10^{-3}	-3.5×10^{-3}	2.7×10^{-3}
I_d/mA	6.5	-5.8	-3.5	2.7

Fig. 5). Hence, the Grimm-type rf discharge appears to have a resistive character for the conditions under study.

Belenguer *et al.*[7] found also that I_d and V differ in phase by $\pi/2$, but because their calculations predicted that I_d is dominant, they found that I and V are out of phase by $\pi/2$, and consequently, that the rf discharge has a capacitive character. However, the experimental measurements reveal that voltage and current are generally in phase with each other in rf glow discharges under typical Grimm-type conditions,[15–17] which indicates the resistive character of analytical Grimm-type rf discharges. The high value of the displacement current calculated in the model of Belenguer *et al.*[7] appears to be related not only to the plasma. Indeed, it appears that they even calculated a high current in the absence of a plasma, where ion and electron conduction currents are of course negligible and only the displacement current without the plasma remains.[18] It is important to emphasize here that the electrical measurements[15–17] refer only to the plasma current, since the capacitive current of the measuring circuit is subtracted from the total current. Without plasma, the remaining current is zero, independent of the voltage. This explains why the experimental data are in agreement with our calculation results and in discrepancy with the calculations of ref. 7.

The product of voltage and current gives the electrical power as a function of time. The latter is presented in Fig. 7, together with the average value of 10.2 W (dashed line), used as input in the model. It appears that the power is positive at all times, because V and I were found to be in phase with each other. This finding is again in good correspondence with the experimental observations,[15–17] and also with the results of our previous model (Fig. 1c in ref. 6).

Summarizing it can be concluded that our improved hybrid Monte Carlo–fluid model yields similar results to our previous hybrid model, except for some minor differences (*e.g.*, in the relative difference between V_{rf} and $V_{dc\text{-}bias}$). However, it should be realized that, in order to reach reasonable values for the voltages (rf amplitude and dc bias) in correspondence with experimental data, a different gas temperature was used in both models, *i.e.*, 1000 K in the previous model, and 700 K in the new model. The reason is that the large amount of alpha-ionization, as it was calculated in the previous fluid model, and which arose from the moderate electric field in the bulk plasma in the previous results[6] (see also above) is not so pronounced in the new model. However, the new value of the gas temperature (700 K) is a realistic value at a power of 10 W,[19] and we believe that the present results are more realistic, because the ionization is treated more correctly in the new rf model.

3.2. Other calculated quantities: electron and argon ion densities, electron, fast argon ion and atom impact ionization rates

Besides having an effect on the gas temperature, the new approach of following all electrons with the Monte Carlo method has some effect on the calculated electron and ion densities, the mean electron energy, and the electron impact ionization rate. Fig. 8 shows the electron density as a function of distance from the rf electrode and at four times in the rf cycle, as calculated in the fluid model. The argon ion density (not shown here) has a similar profile as the electron density at $\omega t = \pi/2$, and is constant as a function of time. The density reaches a maximum at about 2 mm from the rf electrode, which is somewhat further than in the previous model (*ca.* 1 mm). Moreover, the calculated density is also a factor of about 2 higher than in the previous results, which is a consequence of the lower gas temperature, and hence the higher gas density. But beside these differences, which are of the order of the expected uncertainties of the modeling results, the calculated electron density profile, and its variation as a function of time, are similar to our previous results.

The latter cannot be said about the electron impact ionization rate, which is presented in Fig. 9(a), as a function of distance from the rf electrode, and at four times in the rf cycle. It is clear that electron impact ionization is only important at the beginning of the bulk plasma (with a maximum between 1 and 2 mm from the rf electrode) and becomes negligible at distances further than 5 mm from the rf electrode. Moreover, at $\omega t = \pi/2$, electron impact ionization takes place near the rf electrode, because the electrons are

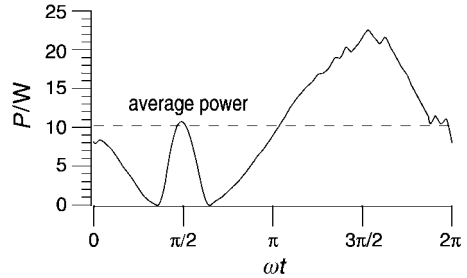

Fig. 7 Calculated electrical power as a function of time in the rf cycle (solid line), for the same discharge conditions as in Fig. 1. The dashed line gives the average power value, used as input in the model (10.2 W).

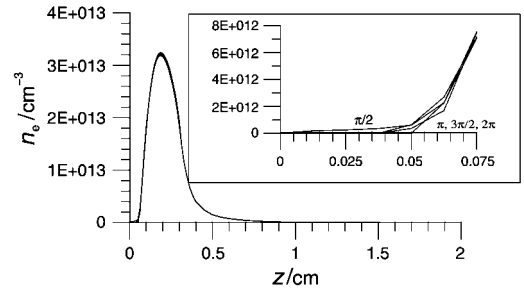

Fig. 8 Calculated electron density profile, at four times in the rf cycle, for the same discharge conditions as in Fig. 1. The enlarged part in the figure shows the behavior in the rf sheath, illustrating that the electron density is zero in the rf sheath at all times, except at $\omega t = \pi/2$.

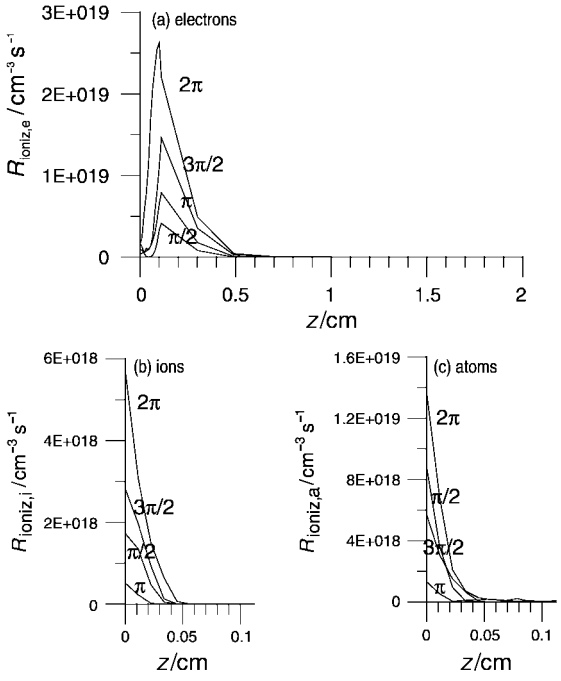

Fig. 9 Calculated electron (a), fast argon ion (b) and fast argon atom (c) impact ionization rates, as a function of distance from the rf electrode, at four times in the rf cycle, for the same discharge conditions as in Fig. 1. Fast argon ion and atom impact ionization are only illustrated in the sheath in front of the rf electrode (note the different x-scales!).

directed toward the rf electrode at this time. Further, it appears that electron impact ionization is highest at $\omega t = 2\pi$, and lowest at $\omega t = \pi/2$. This is in contrast to our previous calculations, where alpha-ionization was calculated in the fluid model to be important at $\omega t = \pi/2$, and especially in the bulk plasma. The latter resulted from the moderate electric field in the bulk plasma at $\omega t = \pi/2$, which yielded, in the fluid model, a mean electron energy just high enough to cause sufficient alpha-ionization, calculated with the empirical formula. In the present modeling results, however, the bulk electric field at $\omega t = \pi/2$ is considerably lower due to a smaller difference between V_{rf} and $V_{dc\text{-}bias}$ (see above), so that this ionization mechanism is less important. Moreover, we believe that the alpha-ionization calculated with the empirical formula in our previous fluid model is too rough an approximation, so that our present results, depicted in Fig. 9(a), are considered much more reliable. Nevertheless, in spite of the major difference in the ionization rate profiles calculated with our previous and the improved hybrid model, it should be mentioned that the other, overall calculation results, and mainly the electrical characteristics, are not much affected.

Finally, Fig. 9(b) and (c) present the fast argon ion and atom impact ionization rates, respectively, as a function of distance from the rf electrode, and at four different times in the rf cycle. Only the sheath in front of the rf electrode is shown, because ion and atom impact ionization is negligible at further distances, where ion and atom energies are too low (indeed, these processes become only important at energies above 100 eV). It appears that both fast argon ion and atom impact ionization are most important at $\omega t = 2\pi$, and are lowest at $\omega t = \pi$. This is because the argon ion and atom energies are highest at $\omega t = 2\pi$, and lowest at $\omega t = \pi$ (because the ions respond to an effective electric field, which is highest at $\omega t = 2\pi$ and lowest at $\omega t = \pi$).[11] Furthermore, it is clear that fast argon ion impact ionization is at least a factor of 5 lower than electron impact ionization, whereas fast atom impact ionization is only a factor of 2 lower. However, although ion and atom impact ionization are lower than electron impact ionization, it should be noted that these processes cannot be neglected in analytical glow discharge models. Indeed, due to these processes, new electrons are created, which give more electron impact ionization; the new ions formed hereby create again more electrons by ion impact ionization and these electrons yield in turn more ionization, *etc.* For example, it was illustrated for the dc glow discharge[20] that, due to this snowball effect, the correct current–voltage characteristics could be predicted, which appeared not to be possible when only electron impact ionization was taken into account.[21]

4. Conclusion

An improved hybrid Monte Carlo–fluid model for argon ions, argon atoms and electrons is developed for an rf analytical Grimm-type glow discharge. The results presented here are the electrical characteristics, including the electric field and potential distribution, the electron and argon ion densities, and the electron, fast argon ion and atom impact ionization rates.

The essential difference with our previous rf hybrid model[6] is that all electrons, including the large slow electron group in the bulk plasma, are treated with the Monte Carlo method, and hence the electron impact ionization is only calculated in the electron Monte Carlo model, which should be more accurate. This results in different electron impact ionization rates, especially at $\omega t = \pi/2$, and also in some differences in the assumed gas temperature and the calculated electron and argon ion densities. However, the calculated electrical characteristics, *i.e.*, voltage, electrical current and power as a function of time in the rf cycle remain essentially the same.

It was demonstrated again that the calculated plasma displacement current is lower than the calculated electron and ion conduction currents. Hence, the calculated electrical current as a function of time in the rf cycle is roughly in phase with the voltage, which indicates the resistive character of the Grimm-type rf discharges. This finding is in agreement with experimental data,[15–17] but is contradictory to the results calculated by Belenguer *et al.*[7] The reason for this inconsistency is that the displacement current calculated in ref. 7 is probably more related to the hardware than to the plasma. However, the experimental measurements in refs. 15–17 focus on the real plasma current (by subtracting the capacitive current of the measuring circuit), and the good agreement with our calculations serves as a validation for our model results.

Acknowledgements

A. Bogaerts is indebted to the Flemish Fund for Scientific Research (FWO) for financial support. The research of W. Goedheer is financed by the "Stichting voor Fundamenteel Onderzoek der Materie". The authors also acknowledge financial support from the Federal Services for Scientific, Technical and Cultural Affairs (DWTC/SSTC) of the Prime Minister's Office through IUAP-IV (Conv. P4/10). Finally, A. Bogaerts wishes to thank L. Pitchford, Ph. Belenguer, P. Miller, V. Hoffmann and L. Wilken, for the interesting discussions during and after the Expert Meeting of the EC Thematic Network on Glow Discharge Spectroscopy for Spectrochemical Analysis (SMT4-CT98-7517), and V. Hoffmann and L. Wilken for supplying the experimental information.

References

1 *Glow Discharge Spectroscopies*, ed. R. K. Marcus, Plenum Press, New York, 1993.
2 *Glow Discharge Optical Emission Spectroscopy*, ed. R. Payling, D. Jones and A. Bengtson, Wiley, Chichester, 1997.
3 V. Hoffmann, H.-J. Uhlemann, F. Praessler, K. Wetzig and D. Birus, *Fresenius' J. Anal. Chem.*, 1996, **355**, 826.
4 P. J. Hargis Jr, K. E. Greenberg, P. A. Miller, J. B. Gerardo, J. J. Van Brunt, M. A. Sobolewski, H. M. Anderson, M. P. Splichnal, J. L. Mock, P. Bletzinger, A. Garscadden, R. A. Gottscho, G. Selwyn, M. Dalvie, J. E. Heidenreich, J. W. Butterbaugh, M. L. Brake, M. L. Passow, J. Pender, A. Lujan, M. E. Elta, D. B Graves, H. H. Sawin, M. J. Kushner, J. T. Verdeyen, R. Horwath and T. R. Turner, *Rev. Sci. Instrum.*, 1994, **65**, 140.
5 A. Bogaerts, R. Gijbels and W. Goedheer, *Jpn. J. Appl. Phys.*, 1999, **38**, 4404.
6 A. Bogaerts, M. Yan, R. Gijbels and W. Goedheer, *J. Appl. Phys.*, 1999, **86**, 2990.
7 Ph. Belenguer, L. C. Pitchford and J. C. Hubinois, *J. Anal. At. Spectrom.*, 2001, **16**, 1.
8 V. Hoffmann, F. Präßler, K. Wetzig, D. Schiel and R. Jährling, *Electrical parameters in Grimm-type glow discharge sources*, Poster at the Winter Conference on Plasma Spectrochemistry, Scottsdale, USA, January 5–10, 1998.
9 V. A. Godyak and A. S. Kanneh, *IEEE Trans. Plasma Sci.*, 1986, **PS-14**, 112.
10 A. Bogaerts, R. Gijbels and W. Goedheer, *Spectrochim. Acta, Part B*, 1999, **54**, 1335.
11 A. Bogaerts and R. Gijbels, *IEEE Trans. Plasma Sci.*, 1999, **27**, 1406.
12 A. Bogaerts, R. Gijbels and W. Goedheer, *Anal. Chem.*, 1996, **68**, 2296.
13 A. Fiala, PhD Dissertation, University Paul Sabatier of Toulouse, Toulouse, 1995.
14 A. Bogaerts and R. Gijbels, *Spectrochim. Acta, Part B*, 1998, **53**, 437.
15 L. Wilken, V. Hoffmann and K. Wetzig, Poster presented at the 10th BNASS, Sheffield, UK, July 17–20, 2000.
16 L. Wilken, V. Hoffmann and K. Wetzig, Lecture presented at the Winter Conference on Plasma Spectrochemistry, Lillehammer, Norway, February 4–8, 2001.
17 A. Bogaerts, L. Wilken, V. Hoffmann, R. Gijbels and K. Wetzig, *Spectrochim. Acta, Part B*, submitted for publication.
18 Ph. Belenguer and L. Pitchford, private communication.
19 A. Bogaerts, R. Gijbels and V. V. Serikov, *J. Appl. Phys.*, 2000, **87**, 8334.
20 A. Bogaerts and R. Gijbels, *J. Appl. Phys.*, 1995, **78**, 6427.
21 A. Bogaerts, R. Gijbels and W. Goedheer, *J. Appl. Phys.*, 1995, **78**, 2233.